HHS Public Access

Author manuscript

J Am Chem Soc. Author manuscript; available in PMC 2021 March 30.

Published in final edited form as:

J Am Chem Soc. 2020 January 29; 142(4): 1987–1994. doi:10.1021/jacs.9b11566.

Self-Assembled Cagelike Receptor That Binds Biologically Relevant Dicarboxylic Acids via Proton-Coupled Anion Recognition

Fei Wang,
Shanghai University, Shanghai, China

Sajal Sen,
The University of Texas at Austin, Austin, Texas

Chuang Chen,
Shanghai University, Shanghai, China

Steffen Bähring,
University of Southern Denmark, Odense M, Denmark

Chuanhu Lei,
Shanghai University, Shanghai, China

Zhiming Duan,
Shanghai University, Shanghai, China

Zhan Zhang,
South-Central University for Nationalities, Wuhan, China

Jonathan L. Sessler,
Shanghai University, Shanghai, China, and The University of Texas at Austin, Austin, Texas

Atanu Jana
Shanghai University, Shanghai, China

Abstract

We report here a fully organic, self-assembled dimeric receptor, constructed from acyclic naphthyridyl–polypyrrolic building blocks. The cagelike dimer is stable in the solid state, in

Corresponding Authors: sbahring@sdu.dk; chlei@shu.edu.cn; zhangzhan5@foxmail.com; sessler@mail.utexas.edu; atanu.j78@gmail.com.

The authors declare no competing financial interest.

Supporting Information
The Supporting Information is available free of charge at https://pubs.acs.org/doi/10.1021/jacs.9b11566.
The experimental procedures and all the characterization data, additional photophysical results, X-ray data, etc. (PDF)
X-ray crystal data of synthon **3** (CIF)
X-ray crystal data of receptor **7•7** (CIF)
X-ray crystal data of the host–guest complex obtained between the supramolecular receptor **7•7** and maleic acid (CIF)
X-ray crystal data of the host–guest complex obtained between the supramolecular receptor **7•7** and oxalic acid (CIF)
X-ray crystal data of host–guest complexation between supramolecular receptor **7•7** and malonic acid (CIF)
X-ray crystal data of the host–guest complex obtained between the supramolecular receptor **7•7** and sulfuric acid (CIF)

Complete contact information is available at: https://pubs.acs.org/10.1021/jacs.9b11566

solution, and in gas phase, as inferred from X-ray diffraction and spectroscopic analyses. This system acts as a receptor for oxalic acid, maleic acid, and malonic acid in the solid state and in THF solution. In contrast, acetic acid, propionic acid, adipic acid, and succinic acid, with pK_a values > ca. 2.8, were not bound effectively within the cagelike cavity. It is speculated that oxalic acid, maleic acid, and malonic acid serve to protonate the naphthyridine moieties of the host, which then favors binding of the corresponding carboxylate anions via hydrogen-bonding to the pyrrolic NH protons. The present naphthyridine–polypyrrole dimer is stable under acidic conditions, including in the presence of 100 equiv trifluoroacetic acid (TFA), *p*-toluenesulfonic acid (PTSA), H_2SO_4, and HCl. However, disassembly may be achieved by exposure to tetrabutylammonium fluoride (TBAF). Washing with water then regenerates the cage. This process of assembly and disassembly could be repeated >20 times with little evidence of degradation. The reversible nature of the present system, coupled with its dicarboxylic acid recognition features, leads us to suggest it could have a role to play in effecting the controlled “capture” and “release” of biologically relevant dicarboxylic acids.

Graphical Abstract

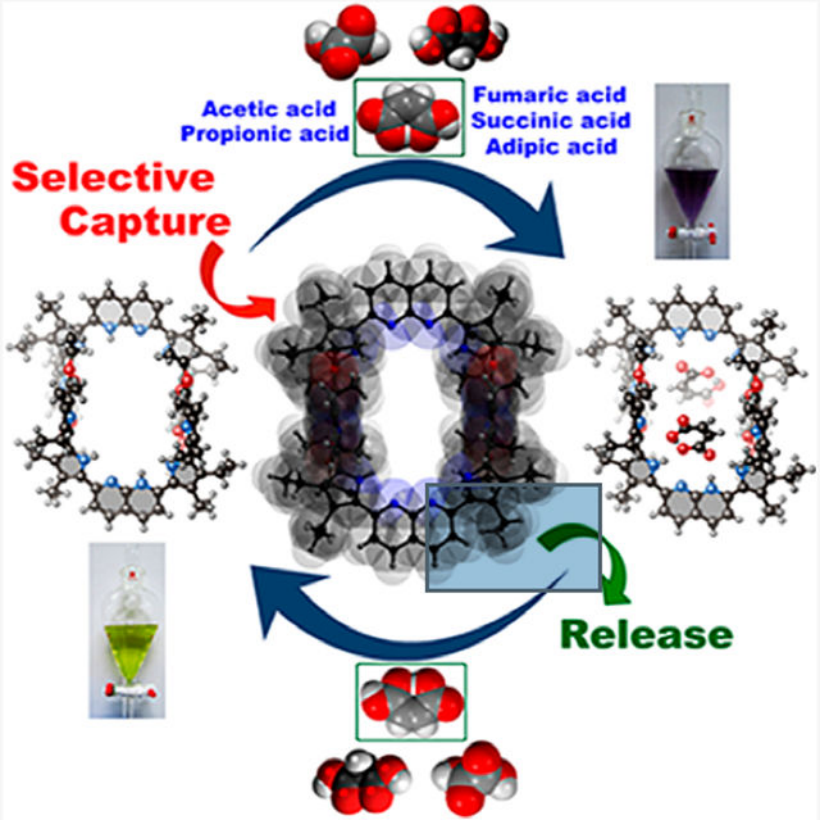

INTRODUCTION

One of the current challenges in supramolecular chemistry is to create receptors that are produced from relatively simple components through self-assembly. Recently, considerable progress has been made in the area of metal-supported cages,[1–6] many of which display

features, including recognition[3,5] and catalysis,[4,6] that are not replicated in the case of receptors prepared through more conventional syntheses. In contrast, the corresponding chemistry in the case of purely organic self-assembled systems is far less well developed. However, a number of elegant systems have been reported where purely organic precursors undergo self-assembly via hydrogen- or halogen-bonding interactions to produce supramolecular receptors for various complementary guests.[7–12] Of particular interest are so-called cages produced through the dimerization of complementary monomers.[7,8,12] To date, self-assembled cages have permitted the effects of solvent-isolated environments to be explored in detail and a range of "chemistry within a cage" studies to be carried out.[13–15] However, at present only a few general classes of cages are known. New cages are thus needed if the full potential of this approach to self-assembled receptor design is to be realized. Here we report a 1,8-naphthyridine-based tetrapyrrolic acyclic synthon (**7**) that is able to create a cagelike macrocyclic dimer through hydrogen-bond driven self-assembly. The resulting construct acts as an effective receptor for oxalic acid, maleic acid, and malonic acid in THF. Selectivity for these biologically relevant dicarboxylic acids is maintained even when other mono- and dicarboxylic acids are present in excess. The present cage is stable in the presence of excess mineral acid (e.g., HCl or H_2SO_4). However, it can be dissociated and reassembled by treatment with TBAF and washing with water, respectively.

Organic dicarboxylic acids play important roles, both favorable and unfavorable, in human physiology.[16–18] For example, oxalic acid is responsible for joint pain and kidney failure through precipitation of calcium oxalate.[19] This makes these dicarboxylic acids important targets for supramolecular chemists.[20,21] However, recognition of such species is made challenging due to their characteristic sizes, shapes, pK_a profiles, and slightly hydrophilic nature. Indeed, there are only a handful of reports of dicarboxylic acid recognition in the literature.[22–27] Exacerbating the problem is the need to account for geometric isomers, e.g., maleic acid (*Z*-isomer) vs fumaric acid (*E*-isomer). As detailed below, we have prepared a cagelike supramolecular receptor **7•7** via the self-assembly of **7** (cf. Scheme 1 and Figure 1). Dimer **7•7** is stabilized by four pyrrole NH-ester oxygen hydrogen-bond interactions. It retains its integrity in acidic media and is able to bind oxalic acid, malonic acid, and maleic acid, effectively in THF, but not fumaric acid and others having pK_a values > ca. 2.8. Binding is achieved as the result of proton-coupled anion recognition within the self-assembled cage. The present supramolecular macrocyclic receptor adds to our understanding of dicarboxylic acid recognition by providing an easy-to-implement approach that provides for high reversibility and selectivity.

RESULTS AND DISCUSSION

The monomer **7** used to create cage **7•7** incorporates bulky ethyl groups on the β-positions of the pyrroles; this creates a sterically crowded environment that enforces an orthogonal arrangement of the terminal pyrrole moieties relative to the mean plane defined by the three central heterocyclic molecules. These terminal pyrroles and their ester functionalities, in turn, promote the formation of the cagelike dimer **7•7**, via C=O···HN hydrogen-bonding interactions involving two neighboring acyclic units of **7**. The result is a pseudorectangular cavity of average inner core diameter of ca. 10 Å, which was judged suitable for small dicarboxylic acid recognition. Support for this latter contention came from solid-state single

crystal X-ray diffraction analyses along with solution phase ^{1}H NMR, UV–vis absorption, and fluorescence spectroscopic titration studies (vide infra).

Synthetic Route to the Acyclic Polypyrrolic Synthon, 7.

The synthesis of the 1,8-naphthyridine-appended acyclic tetrapyrrolic receptor, **7**, is summarized in Scheme 1. The key precursor, **1**, was synthesized in accord with a literature procedure.[28] Precursor **3** was prepared via a Pd(II)-acetatecatalyzed Suzuki–Miyaura cross-coupling reaction using commercially available 2,7-dibromo-1,8-naphthyridine, **2**, following a literature report.[29] Subjecting **3** to hydrolysis using aqueous NaOH, followed by high temperature decarboxylation of the resulting intermediate **4**, yielded the reactive α-free dipyrrole **5**. Iodination of **5** at both terminal α-pyrrolic positions gave **6**, which was then subjected to a Pd(0)-catalyzed Suzuki–Miyaura cross-coupling reaction to give **7** in overall good yield.

All new compounds were fully characterized by ^{1}H and ^{13}C NMR spectroscopy, as well as mass spectrometric analysis. The structure of **7** was confirmed via a single crystal X-ray diffraction analysis (vide infra); this revealed formation of a self-assembled dimer (**7•7**) in the solid state. Evidence that a dimeric form was retained in solution and in the gas phase came from an analysis of the ESI-TOF mass spectrum (see Figure S16 in Supporting Information).

X-ray Diffraction Analyses.

Crystallographic data have been deposited in the Cambridge Crystallographic Data Centre (CCDC) under reference numbers CCDC-1937460, 1937464, 1951161, 1951162, 1951163, and 1951164. Single crystals suitable for X-ray diffraction analysis were grown either from THF or $CHCl_3$ solutions of **7**, diffused with hexanes (cf. Supporting Information for further details). Analysis of the resulting structure revealed that the diethylpyrrole subunits attached to the central 1,8-naphthyridine are coplanar (cf. Figure 1a). However, the two terminal diethylpyrrole moieties are almost perpendicular to the mean plane containing the 1,8-naphthyridine and its two adjacent diethylpyrroles (Figure 1a). This latter distortion is attributed to the presence of sterically hindered ethyl groups on the β-positions of all four pyrrole units. In the event, a conformation is established for **7•7** (Figures 1b,c) that is preorganized for the formation of a hydrogen-bonded supramolecular cagelike structure. Analysis of the space filling model of the self-assembled structure, **7•7**, revealed a large rectangular inner cavity (Figure 1d). The “total potential solvent occupied void volume” calculated using the PLATON crystallographic software[30] was found to be ca. 825 Å^3 (or ca. 30% of the per unit cell volume of 2692 Å^3). Meanwhile, the presence of two basic 1,8-naphthyridine units (pK_{a1} of 1,8-naphthyridine = 3.39 in aqueous media) within this supramolecular cavity led us to envision that this self-assembled cage might provide an environment suitable for acidic substrate recognition, including mono- or dicarboxylic acid guests.

Diffraction grade single crystals of the key precursor, **3**, could also be obtained. In this case, the resulting structure (Figure 1e) did not reveal a system appropriately oriented for the formation of a cagelike dimer. Rather, precursor **3** exists in the form of a one-dimensional

infinite linear/zigzag hydrogen-bonded network(**3**)$_n$ in the solid state (cf. Figure 1f). A comparison of these two solid-state X-ray structures, (**3**)$_n$ vs **7•7**, reveals the preorganizational benefits provided by the two sterically crowded terminal esterified pyrroles in the case of **7**. However, it is important to appreciate that, as crystallized **7•7** encapsulates four $CHCl_3$ solvent molecules as guests (cf. Figure 2a).

Given the above structural insights, an effort was made to test whether **7•7** could act as a receptor for mono- and dicarboxylic acids of biological and environmental interest. Specifically, we tested acetic acid (pK_a = 4.76 in water), TFA (pK_a = 0.23 in water), propionic acid (pK_a = 4.88 in water), oxalic acid (pK_{a1} = 1.24 in water), maleic acid (pK_{a1} = 1.90 in water), malonic acid (pK_{a1} = 2.83 in water), fumaric acid (pK_{a1} = 3.03 in water), succinic acid (pK_{a1} = 4.20 in water), and adipic acid (pK_{a1} = 4.43 in water). These species provide a sampling of size, geometries, and pK_a values. As detailed below, receptor **7•7** was found to accommodate small dicarboxylic acids as their monocarboxylate anions (e.g., hydrogen oxalate (Hoxalate$^-$), hydrogen maleate (Hmaleate$^-$), and hydrogen malonate (Hmalonate$^-$), respectively) following proton transfer. As inferred from X-ray structural analyses and spectroscopic studies, carboxylic acids having pK_a values < ca. 2.8 protonate the naphthyridine N atoms; this creates a positively charged environment inside the cavity suitable for carboxylate anion recognition. However, acids having pK_a values higher than 2.8 were found not to interact with this receptor. On the basis of a suggestion of a reviewer, larger acids having pK_a values ≤2.8, e.g., 4,4′-biphenyldisulfonic acid (BPDSA, pK_{a1} = −3.0), tetraphenylporphyrin tetrasulfonic acid (TPPTSA, pK_{a1} = −2.10) were also tested as potential substrates. Again, a combination of ^{1}H NMR, UV–vis, and fluorescence spectroscopic analyses revealed evidence of binding (cf. Figures S32, S40, and S45). Although the specific nature of the resulting complexes could not be determined from these studies, these findings were taken as evidence that the pK_a of the acids plays an important role in defining the molecular recognition features of **7•7**.

A single crystal X-ray diffraction analysis of **7•7** cocrystallized with maleic acid revealed that each naphthyridine unit is singly protonated. A maleate anion interacts with this protonated naphthyridine unit and benefits from hydrogen bonding interactions involving the inner pyrrolic NH protons. These combined effects result in encapsulation of two maleate anions within the cavity of receptor **7•7** (see Figure 2b). Analysis of the crystal packing diagram reveals a one-dimensional (1D) stacking of the maleic acid guests within an infinite tunnel created by close-packed hosts (Figure 2e). Similar proton-coupled carboxylate anion recognition was observed in the case of oxalic acid, pK_{a1} = 1.24 in water (Figure 2c) and malonic acid, pK_{a1} = 2.83 in water (Figure 2d). However, in the case of oxalic acid and malonic acid, two additional THF solvent molecules are found within the cavity; they bridge between two entrapped oxalic/malonic acids via hydrogen-bonding interactions. Unfortunately, efforts to grow diffraction-grade single crystals with other mono- and dicarboxylic acids proved unsuccessful. This was taken as an initial indication that such species are unable to form stable host–guest complexes with **7•7**.

Exposing CH2C2 solutions of the above host–guest complexes to aqueous environments serves to release the carboxylic acid guests. In the case of oxalic acid, a distinctive visual color change from deep bluish-violet to canary yellow is seen upon guest release (Figure

S18). After this aqueous treatment, receptor **7•7** was recovered from the organic layer as inferred from ^{1}H NMR spectroscopic studies (Figure S19c). A similar observation was seen in the case of PTSA (Figure S20). These findings lead us to suggest that receptor **7•7** could capture effectively a target guest molecule in an organic phase and then release it into an aqueous collection medium. In fact, in the case of oxalic acid this process of guest capture and release could be carried out for more than 20 cycles without evidence of appreciable degradation of **7•7**. It is worth noting that both tetrabutylammonium oxalate and tetrabutylammonium hydrogen sulfate salts are unable to interact with receptor **7•7**; presumably, this reflects an inability of these species to protonate the naphthyridine moieties (Figure S21a,b).

In an effort to dissociate the self-assembled cage system composed of **7•7** in THF, the strong acids PTSA, H_2SO_4, and HCl were added in excess. It was noticed that, even in the presence of 100 equiv of these representative strong acids, the dimeric form of the self-assembled cage remains intact as inferred from the X-ray structure of receptor **7•7** with H_2SO_4 (Figure 3). The overall geometry of this host–guest complex mirrors what was observed for cage **7•7** in the presence of other dicarboxylic acids (cf. Figure 2).

^{1}H NMR Spectroscopic Titrations.

To understand the dynamics of host–guest complexation in solution, ^{1}H NMR spectroscopic titrations and ^{1}H DOSY NMR experiments were performed with various mono- and dicarboxylic acids in THF-d_8 at 298 K. Upon the incremental addition of 100 equiv of oxalic acid, maleic acid, and malonic acid to the host solution, a gradual downfield shift in the inner pyrrolic NH proton signal at 10.55 ppm to ca. 11.82 ppm occurs ($\Delta\delta$= 1.27 ppm) (see Figure S22a–c). This is taken as evidence that significant host–guest interactions between these dicarboxylic acid substrates and cage **7•7** are being established under the conditions of these experiments. On the other hand, the terminal pyrrolic NH proton signal at 10.75 ppm remains unshifted. Therefore, we infer that this particular proton does not play a substantial role in substrate recognition. Rather, we suggest that it interacts with the ester carbonyl groups of the other subunit making up the cage. Because these latter hydrogen-bonding interactions are not perturbed by substrate binding, the terminal NH proton signal remains relatively unchanged during the course of the titration. This is as expected for a self-assembled dimer, namely cage **7•7**, that retains its integrity during the course of these experiments.

Similar changes in the ^{1}H NMR spectral features were seen when receptor **7•7** was titrated against TFA (pK_a = 0.23 in water) (cf. Figure S22d). In contrast, the signals at both 10.55 and 10.75 ppm remained unshifted when the host was titrated against fumaric acid, adipic acid, succinic acid, acetic acid, and propionic acid. We thus infer that no substantial host–guest complexation is occurring in the latter instances (Figures S23a–d and S24a). This absence of apparent binding may reflect their larger molecular dimensions and relatively higher pK_a values (>2.8 in water) as compared to oxalic acid, maleic acid, and malonic acid.

When the receptor was titrated against PTSA, a comparatively small shift in the NH signal at 10.75 ppm was seen ($\Delta\delta$ = 0.2 ppm). However, the inner pyrrolic NH signal at 10.55 ppm underwent a significant downfield shift to 12.53 ppm ($\Delta\delta$ = 1.98 ppm) (Figure 4a). This

mirrors what was seen for oxalic acid, maleic acid, and malonic acid and was likewise taken as evidence of an appreciable host–guest interaction. Other relatively strong acids, e.g., H_2SO_4 ($pK_a = -3.0$ in water) and HCl ($pK_a = -6.3$ in water) induce similar spectral changes Figure S25a,b. Specifically, no significant change in the chemical shift of the terminal NH signal at 10.75 ppm was seen in the presence of 100 equiv of various strong acids. Again, this was taken as evidence that cage **7•7** remains largely intact in the presence of these representative strong acids (cf. Figures S30e, S31a,b, and S32a,b, respectively).

After titrating with various acidic substrates, the pristine dimeric cage **7•7** can be recovered by washing with water, as inferred from ^{1}H NMR spectroscopic analyses (cf. Figure 4a). However, the addition of tetrabutylammonium fluoride (TBAF) effectively disintegrates the cage (Figure 4b). Presumably, this disassembly is driven by strong interactions between the F^- anion and the pyrrolic NH groups. In the limit, these interactions can lead to deprotonation of the pyrrolic NH groups with concomitant generation of HF_2^- species. Low temperature ^{1}H NMR spectroscopic experiments carried out in THF-d_8 revealed the characteristic HF_2^- signal at 15.85 ppm (Figure S27d,e). Subjecting this latter sample to an aqueous wash led to the regeneration of the dimeric cage, as inferred from the ^{1}H NMR spectrum (Figure 4b).

A degree of disassembly can also be induced by TBACl but to a far lesser extent on a per equivalent basis as compared to TBAF (Figure 4c). Again, the induced disassembly produced by this weaker Lewis basic anion is ascribed to the interaction between the added Cl^- anions and the pyrrolic NH protons, which competes with the dimer-forming interactions between two molecules of **7**. This chemistry stands in contrast to what is seen for the corresponding acid (i.e., HCl) and reflects the difference in receptor protonation state. Addition of $AgNO_3$, which presumably serves to remove the chloride anions in the form of AgCl(s), leads to reformation of the self-assembled dimer (i.e., cage **7•7**) (cf. Figure 4c). Therefore, the supramolecular receptor **7•7** can be reversibly disassembled and reassembled by means of appropriately chosen chemical inputs (addition of F^-, Cl^-, and Ag^+) or through an aqueous wash.

Competition experiments were performed wherein receptor **7•7** was tested for its ability to complex oxalic acid, in the presence of 100 equiv of either propionic acid or fumaric acid (Figure S28a,b). In the case of both putative inhibitors, which are taken as being representative of other biologically relevant mono- and dicarboxylic acids, chemical shifts were produced that are similar to what were seen when the same titration was carried out using pristine oxalic acid (Figure S22a). These experiments provide support for the conclusion that receptor **7•7** binds oxalic acid well, even in the presence of a 100-fold excess of propionic acid or fumaric acid.

^{1}H DOSY NMR spectroscopic analysis of pristine receptor **7•7** in THF-d_8 at 298 K proved consistent with the presence of a single dominant species (see Figure S34a) with a diffusion coefficient of ca. $5.98 \pm 0.1 \times 10^{-6}$ cm^2 s^{-1}. This allowed an effective solvodynamic radius of 7.98 ± 0.07 Å to be calculated.[31] This latter value is in agreement with the average radius for **7•7** determined from the single crystal X-ray structural data (ca. 8.1 Å). This concordance supports the conclusion that receptor **7** exists predominantly in the form of a

dimeric cage in solution. In the presence of 20 equiv of TBAF, a diffusion coefficient of ca. $4.52 \pm 0.15 \times 10^{-6}$ cm^2 s^{-1} is obtained. This value is thought to reflect the presence of relatively larger species (with an effective radius of ca. 11 Å) in the medium. These species are considered to be fluoride-induced deprotonated forms (i.e., $\mathbf{7}^{n-}$, where $n = 1, 2, 3$, etc.; cf. Figure S27d,e) to which the TBA^+ counter cations are associated.

In the case of weaker acids, e.g., fumaric acid, no significant change in the diffusion coefficient value relative to the free host **7•7** was seen under otherwise identical experimental conditions (Figure S34b). Such a finding is consistent with the suggestion that such species do not bind to host **7•7** and thus do not perturb its effective solvodynamic radius.

To confirm that the observed spectral changes are directly related to guest binding, a ^1H DOSY NMR titration with PTSA in THF-d_8 at 298 K was performed as a representative example (see Figure S36a–e). It was found that upon addition of 1 equiv of PTSA to a 10 mM solution of host **7•7**, the diffusion coefficient ($5.79 \pm 0.2 \times 10^{-6}$ cm^2 s^{-1}) proved similar to that recorded for the pristine host ($5.56 \pm 0.3 \times 10^{-6}$ cm^2 s^{-1}) (see Table S2 for details). Taken in concert with the ^1H NMR spectroscopic titration studies discussed above, this experimental result provides support for the conclusion that the presumed host–guest interactions take place within the cagelike cavity of **7•7**, as opposed to some other mode, such as outside binding or a generalized aggregation, which would be expected to lead to discernible changes in the diffusion coefficients.

UV–vis Spectroscopic Titrations.

To understand the determinants of guest binding, steady-state absorption spectroscopic titrations were carried out with cage **7•7** using various mono- and dicarboxylic acids as potential guests in anhydrous THF at 298 K. Gradual addition of oxalic acid or maleic acid to the receptor **7•7** led to modest hypochromic changes in the absorption maxima (λ_{max} = 440 nm) along with the concomitant appearance of a new band centered at 560 nm (Figure 5a,b). The presence of an isosbestic point at ca. 468 nm was also seen. These spectroscopic changes were correlated with readily observable color changes from light yellow (pristine host **7•7**) to bluish-violet (in the presence of these dicarboxylic acid guests) (cf. Figure 5a,b, inset). Despite the apparently clean spectral conversion, efforts to fit the changes to simple binding models failed. Rather, they revealed normalized changes in absorption vs added guest that varied with wavelength. This reflects the complexity of the overall equilibrium process that involves both cage protonation and anion binding, as well as possibly disassociation of hydrogen-bonded dicarboxylic acid dimers and oligomers.

Similar, but discernibly different, photophysical phenomena were observed when receptor **7•7** was titrated with TFA, PTSA, H_2SO_4, HCl, BPDSA, and TPPTSA (Figures S38–S40). However, titrations with relatively weaker acids gave rise to much smaller spectroscopic changes (cf. Figure S41a–d). Finally, distinctive spectral features were observed when the cagelike receptor **7•7** was titrated with TBAF (Figure 5d). Such a finding provides additional support for the suggestion initially made on the basis of the ^1H NMR spectroscopic studies that deprotonation of the pyrrolic NH protons takes place; this leads to a new species having a λ_{max} at 464 nm.

Fluorescence Spectroscopic Titrations.

In an effort to gain additional insight into the structure–property relationships governing anion recognition and the effect of guest-binding on host **7•7**, steady-state fluorescence spectroscopic titrations were performed in anhydrous THF at 298 K. It was observed that the receptor-based emission intensity (λ_{max} = 516 nm)[32,33] was significantly quenched when cage **7•7** was titrated against oxalic acid, maleic acid, or malonic acid (Figure 6a–c). This is presumably due to the photoinduced electron transfer (PET) occurring within these individual host–guest combinations. Strong acids (e.g., TFA, PTSA, H_2SO_4, HCl, BPDSA, and TPPTSA) give rise to similar quenching of the emission intensity when tested under identical experimental conditions (Figures S43–S45). Likewise, an emission quenching was observed when the cage was titrated against TBAF (Figure 6d). A much weaker quenching effect was seen when **7•7** was titrated against TBACl (Figure S46). No visible change in the emission intensities was observed when the receptor was titrated against excess (1000 equiv) of various weak mono- and dicarboxylic acids with pK_a values > ca. 2.8 (Figure S47).

The emission quenching data from the fluorescence titration of **7•7** with oxalic acid could be fitted to either a standard 1:1 or 1:2 statistical binding equation using the BindFit software.[34] This gave values of $K = 1.0 \times 10^4$ M^{-1}, $K_1 = 2.1 \times 10^4$ M^{-1}, and $K_2 = 5.2 \times 10^3$ M^{-1}, respectively, with 4.3% fitting errors in both cases (Figure S48a,b). Similar fittings could be made in the case of maleic acid and sulfuric acid, with the standard 1:1 and statistical 1:2 equations yielding equally good fits in both cases ($K = 4.90 \times 10^3$ M^{-1}; $K_1 = 9.8 \times 10^3$ M^{-1}; $K_2 = 2.4 \times 10^3$ M^{-1} (5.8% fitting error) and $K = 2.6 \times 10^5$ M^{-1}; $K_1 = 7.0 \times 10^5$ M^{-1}; $K_2 = 1.8 \times 10^5$ M^{-1} (6.8% fitting error) for maleic and sulfuric acid, respectively; cf. Figure S48c–f). However, the complexity of the system, involving a putative combination of protonation and anion binding effects, as well as break up of possible hydrogen-bonded dicarboxylate dimers and aggregates in the case of the dicarboxylic acids, precludes assignment of these numerical *K*-values to any specific underlying physical model, such as carboxylic acid disaggregation, cage mono- or diprotonation, or subsequent/concurrent anion binding.[35]

CONCLUSIONS

A new acyclic polypyrrolic system was synthesized that forms a supramolecular cage (**7•7**) as the result of quadruple hydrogen-bonding interactions involving the dimerization of two individual acyclic units of **7**. This cage retains its dimeric form in the solid, liquid, and gaseous states and is stable under acidic condition. Host–guest complexation studies of this cage using various biologically relevant mono- and dicarboxylic acids revealed selectivity for oxalic, maleic, and malonic acids in THF relative to weaker organic acids. Evidence for binding strong mineral acids was also seen. The ability to form these proposed host–guest complexes in the solid state was confirmed by means of single crystal X-ray structures and supported by solution-state studies. The reversible formation of receptor **7•7** and its ability to form supramolecular complexes that may be disassembled and reassembled via chemical means (e.g., fluoride anion treatment; aqueous washing) leads us to suggest that the present all-organic supramolecular cage could potentially be used as a “capture and release” host system for various biologically relevant small dicarboxylic acids.

Supplementary Material

Refer to Web version on PubMed Central for supplementary material.

ACKNOWLEDGMENTS

We thank Shanghai University (N-13-G210-19-214) for providing infrastructure and facilities. This work was supported by the Eastern Scholars program from the Shanghai Municipal Education Committee and the National Natural Science Foundation of China (no. 21901155 to C.L.), a Grant-in-Aid (no. 20108010 to Z.Z.), and the National Natural Science Foundation of China (grant 21672141 to Z.Z.). We thank the staff of Beamline BL17B at the National Facility for Protein Science Shanghai and Shanghai Synchrotron Radiation Facility for assistance during the single crystal X-ray data collection. The work in Austin was supported by the National Institutes of Health (GM RO1 103790 to J.L.S.) and the Robert A. Welch Foundation (F-0018 to J.L.S.). We thank Prof. Julius Rebek, Jr., for kindly looking over an early version of this manuscript. We express our appreciation to the referees for their valuable suggestions.

REFERENCES

(1). Fujita M; Tominaga M; Hori A; Therrien B Coordination Assemblies from a Pd(II)-Cornered Square Complex. Acc. Chem. Res 2005, 38, 369–378. [PubMed: 15835883]

(2). De S; Mahata K; Schmittel M Metal-coordination-drivendynamic heteroleptic architectures. Chem. Soc. Rev 2010, 39, 1555–1575. [PubMed: 20419210]

(3). Saha ML; Yan X; Stang PJ Photophysical Properties of Organoplatinum(II) Compounds and Derived Self-Assembled Metallacycles and Metallacages: Fluorescence and Its Applications. Acc. Chem. Res 2016, 49, 2527–2539. [PubMed: 27736060]

(4). Ueda Y; Ito H; Fujita D; Fujita M Permeable Self-Assembled Molecular Containers for Catalyst Isolation Enabling Two-Step Cascade Reactions. J. Am. Chem. Soc 2017, 139, 6090–6093. [PubMed: 28402111]

(5). Chang X; Zhou Z; Shang C; Wang G; Wang Z; Qi Y; Li Z-Y; Wang H; Cao L; Li X; Fang Y; Stang PJ Coordination-Driven Self-Assembled Metallacycles Incorporating Pyrene: Fluorescence Mutability, Tunability, and Aromatic AmineSensing. J. Am. Chem. Soc 2019, 141, 1757–1765. [PubMed: 30608681]

(6). Cullen W; Takezawa H; Fujita M Demethylenation of Cyclopropanes via Photoinduced Guest-to-Host Electron Transfer in an M_6L_4 Cage. Angew. Chem., Int Ed 2019, 58, 9171–9173.

(7). Ballester P; Gil-Ramírez G Self-assembly of Dimeric Tetraurea Calix[4]pyrrole Capsules. Proc. Natl. Acad. Sci. U. S. A 2009, 106, 10455–10459. [PubMed: 19261848]

(8). Jiang W; Rebek J Jr. Guest-Induced, Selective Formation of Isomeric Capsules with Imperfect Walls. J. Am. Chem. Soc 2012, 134, 17498–17501. [PubMed: 23062190]

(9). Metrangolo P; Meyer F; Pilati T; Resnati G; Terraneo G Halogen Bonding in Supramolecular Chemistry. Angew. Chem., Int. Ed 2008, 47, 6114–6127.

(10). Metrangolo P; Neukirch H; Pilati T; Resnati G Halogen Bonding Based Recognition Processes: a World Parallel to Hydrogen Bonding. Acc. Chem. Res 2005, 38, 386–395. [PubMed: 15895976]

(11). Ajami D; Liu L; Rebek J Jr. Soft Templates in Encapsulation Complexes. Chem. Soc. Rev 2015, 44, 490–499. [PubMed: 24705709]

(12). Zhang K-D; Ajami D; Rebek J Jr. Hydrogen-bonded Capsules in Water. J. Am. Chem. Soc 2013, 135, 18064–18066. [PubMed: 24245649]

(13). Ajami D; Rebek J Jr. More Chemistry in Small Space. Acc. Chem. Res 2013, 46, 990–999. [PubMed: 22574934]

(14). Wu N-W; Rebek J Jr. Cavitands as Chaperones for Monofunctional and Ring-Forming Reaction in Water. J. Am. Chem. Soc 2016, 138, 7512–7515. [PubMed: 27259017]

(15). Shi Q; Masseroni D; Rebek J Jr. Macrocyclization of Folded Diamines in Cavitands. J. Am. Chem. Soc 2016, 138, 10846–10848. [PubMed: 27529442]

(16). Yang X; Cai S; Liu X; Chen P; Zhou J; Zhang H Design, Synthesis and Biological Evaluation of 2,5-Dimethylfuran-3-Carboxylic Acid Derivatives as Potential IDO1 Inhibitors. Bioorg. Med. Chem 2019, 27, 1605–1618. [PubMed: 30858027]

(17). Lund J; Aas V; Tingstad RH; Van Hees A; Nikolić N Utilization of Lactic Acid in Human Myotubes and Interplay with Glucose and Fatty Acid Metabolism. Sci. Rep 2018, 8, 9814. [PubMed: 29959350]

(18). Gajos G Omega-3 Polyunsaturated Fatty Acids in Patients with Coronary Disease Treated with Percutaneous Coronary Intervention. In Handbooks of Lipids in Human Functions; Elsevier Inc., 2016; Chapter 11, pp 319–329.

(19). Pandey V; Singh M; Pandey D; Kumar A Integrated Proteomics, Genomics, Metabolomics Approaches Reveal Oxalic Acid as Pathogenicity Factor in *Tilletia Indica* Inciting Karnal Bunt Disease of Wheat. Sci. Rep 2018, 8, 7826. [PubMed: 29777151]

(20). McLain SE; Soper AK; Watts A Structural Studies on the Hydration of L-Glutamic Acid in Solution. J. Phys. Chem. B 2006, 110, 21251–21258. [PubMed: 17048953]

(21). Lim JYC; Marques I; Félix V; Beer PD A Chiral Halogen-Bonding [3]Rotaxane for the Recognition and Sensing of Biologically Relevant Dicarboxylate Anions. Angew. Chem., Int. Ed 2018, 57, 584–588.

(22). Goodman MS; Hamilton AD; Weiss J Self-Assembling, Chromogenic Receptors for the Recognition of Dicarboxylic Acids. J. Am. Chem. Soc 1995, 117, 8447–8455.

(23). Takeuchi M; Imada T; Shinkai S A Strong Positive Allosteric Effect in the Molecular Recognition of Dicarboxylic Acids by a Cerium(IV) Bis[tetrakis(4-pyridyl)-porphyrinate] Double Decker. Angew. Chem., Int. Ed 1998, 37, 2096–2099.

(24). Disch JS; Staples RJ; Concolino TE; Haas TE; Rybak-Akimova EV Nickel(II) Cyclidenes with Appended Ethylpyridine Receptor Centers as Molecular Tweezers for Dicarboxylic Acids. Inorg. Chem 2003, 42, 6749–6763. [PubMed: 14552627]

(25). Ikeda T; Hirata O; Takeuchi M; Shinkai S Highly Enantioselective Recognition of Dicarboxylic Acid Substrates by the Control of Nonlinear Responses. J. Am. Chem. Soc 2006, 128, 16008–16009. [PubMed: 17165733]

(26). Zhang Z; Kim DS; Lin C-Y; Zhang H; Lammer AD; Lynch VM; Popov I; Miljanić OŠ; Anslyn EV; Sessler JL Expanded Porphyrin-Anion Supramolecular Assemblies: Environmentally Responsive Sensors for Organic Solvents and Anions. J. Am. Chem. Soc 2015, 137, 7769–7774. [PubMed: 25965790]

(27). Kusukawa T; Inoue K; Obata H; Mura R Dicarboxylic Acid Recognition of 1,8-bis(N,N'-diethylamidino) Anthracene: NMR, X-ray, ESI-mass and Fluorescence Analyses of Dicarboxylic Acid Binding Complexes. Tetrahedron 2017, 73, 661–670.

(28). Setsune J-I; Toda M; Watanabe K; Panda PK; Yoshida T Synthesis of bis(Pyrrol-2-yl) Arenes by Pd-Catalyzed Cross Coupling. Tetrahedron Lett. 2006, 47, 7541–7544.

(29). Zhang Z; Lim JM; Ishida M; Roznyatovskiy VV; Lynch VM; Gong HY; Yang X; Kim D; Sessler JL Cyclo [m] Pyridine [n] Pyrroles: Hybrid Macrocycles that Display Expanded π-Conjugation upon Protonation. J. Am. Chem. Soc 2012, 134, 4076–4079. [PubMed: 22332703]

(30). Spek AL PLATON SQUEEZE: a Tool for the Calculation of the Disordered Solvent Contribution to the Calculated Structure Factors. Acta Crystallogr., Sect. C: Struct. Chem 2015, 71 (1), 9–18. [PubMed: 25567569]

(31). The effective solvodynamic radius was measured by using Stokes–Einstein equation: $D = k_B T/6// r_S$, considering hard spheres moving in a continuum fluid and neglecting all contributions from solvation and other secondary interactions like ion-pair interactions.

(32). Wang D-H; Zhang Y; Gong Z; Sun R; Zhao D-Z; Sun C-L 1,8-Naphthyridine-based Molecular Clips for Off–On Fluorescence Sensing of Zn^{2+} in Living Cells. RSC Adv. 2015, 5, 50540–50543.

(33). Nishizawa S; Yoshimoto K; Seino T; Xu C-Y; Minagawa M ; Satake H; Tong A; Teramae N Fluorescence Detection of Cytosine/Guanine Transversion Based on a Hydrogen Bond Forming Ligand. Talanta 2004, 63, 175–179. [PubMed: 18969416]

(34). http://www.supramolecular.org.

(35). In the case of H_2SO_4 $K_1 = 1.24 \times 10^5\ M^{-1}$; $K = 3.09 \times 10^4\ M^{-1}$ (0.7% fitting error) was derived by fitting the absorption titration data to a statistical 1:2 model (Figure S49). Although these values are of the same order of magnitude as those derived from the fluorescence quenching

experiments, the 10× difference in concentration, along with complexity of the system under consideration, precludes a direct numerical comparison between these sets of results.

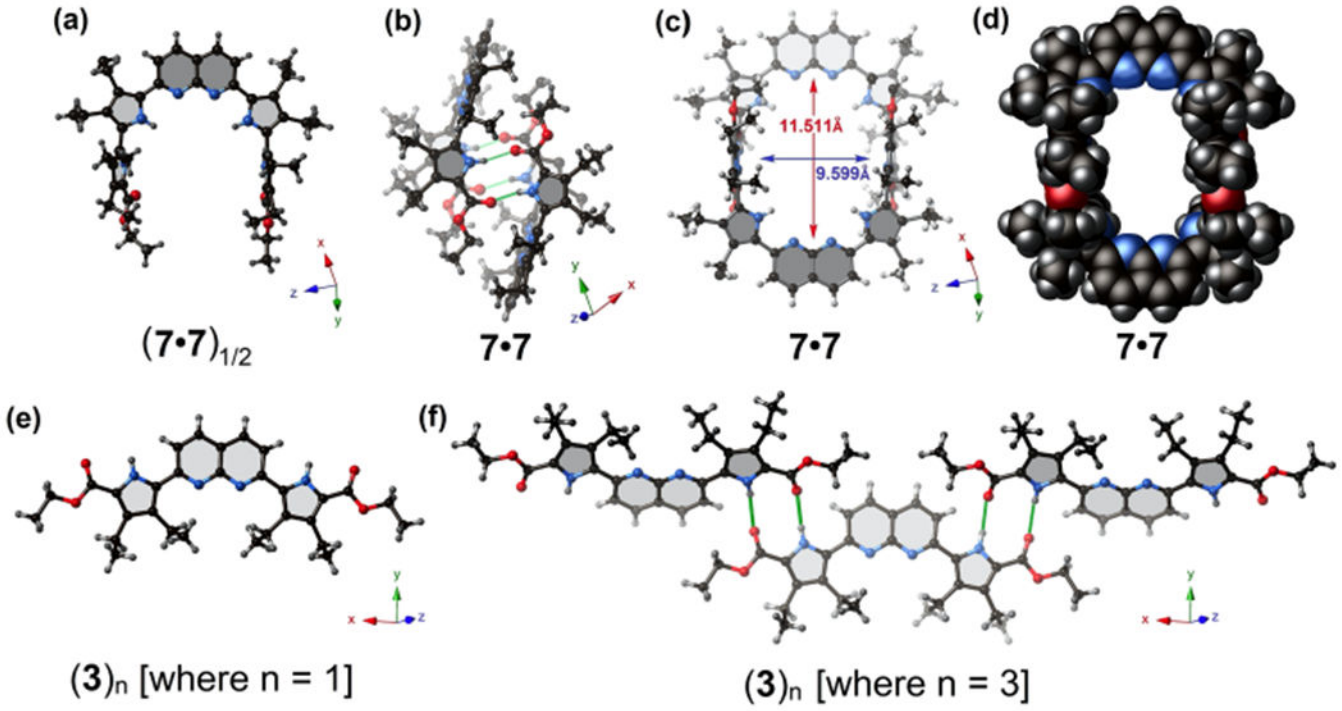

Figure 1.

Single crystal X-ray structures of the acyclic polypyrrolic synthon (**7•7**)$_{1/2}$, along with its corresponding supramolecular macrocyclic receptor, **7•7**. (a) Ball and stick model of a single unit of 7, as present in **7•7**. (b, c) Two different views of the hydrogen-bonded supramolecular dimer **7•7**. (d) Space-filling model of the self-assembled cage **7•7** showing the potential substrate-accessible void. Solvent molecules ($CHCl_3$) are omitted for clarity. (e) Ball and stick model of a single unit of **3**. (f) Truncated view along the crystallographic *z* axis of the infinite hydrogen-bonded "zigzag" supramolecular construct formed by **3** in the solid state, i.e., (3)$_n$. Green lines denote presumed hydrogen-bond interactions between the pyrrolic ester groups and the pyrrole NH protons.

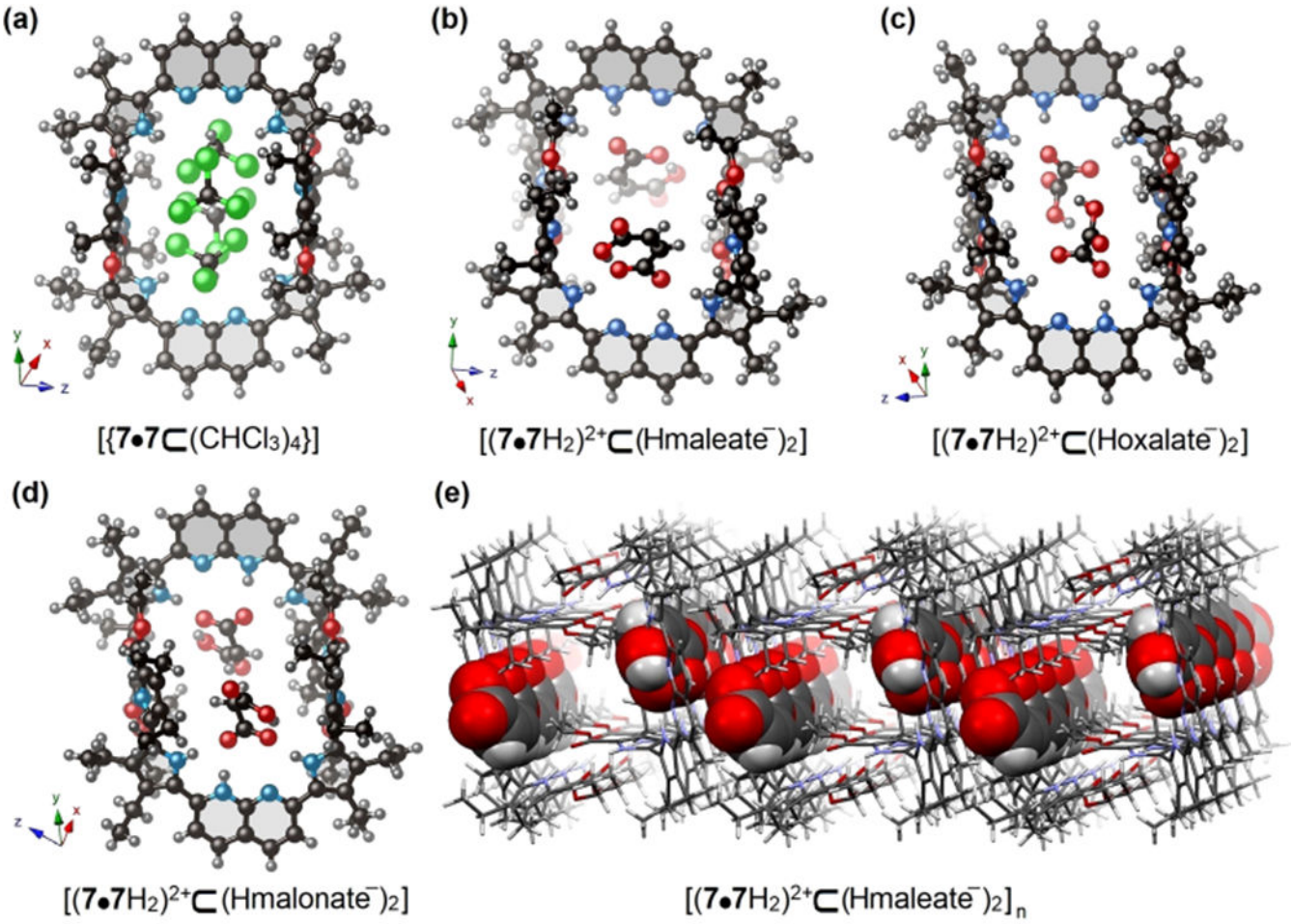

Figure 2.

Single crystal X-ray structures of the hydrogen-bonded dimeric receptor **7•7** and its various host–guest complexes. (a) The illustrative example of host–guest complex between supramolecular receptor **7•7** and $CHCl_3$ with empirical chemical formula [**7•7**⊂$(CHCl_3)_4$]. (b–d) The host–guest complexes between supramolecular receptor **7•7** and maleic acid, oxalic acid, and malonic acid, with empirical chemical formulas [(**7•7**H_2)$^{2+}$⊂$(Hmaleate^-)_2$], [(**7•7**$_2$)$^{2+}$⊂$(Hoxalate^-)_2$], and [(**7•7**H_2)$^{2+}$⊂$(Hmalonate^-)_2$], respectively. Encapsulated THF solvent molecules are omitted for clarity. (e) A representative example of 3D packing of maleic acid guests within the cavities of **7•7** along the crystallographic *x* axis. Note: The entrapped guests within the cavity are shown in space-filling form in (e).

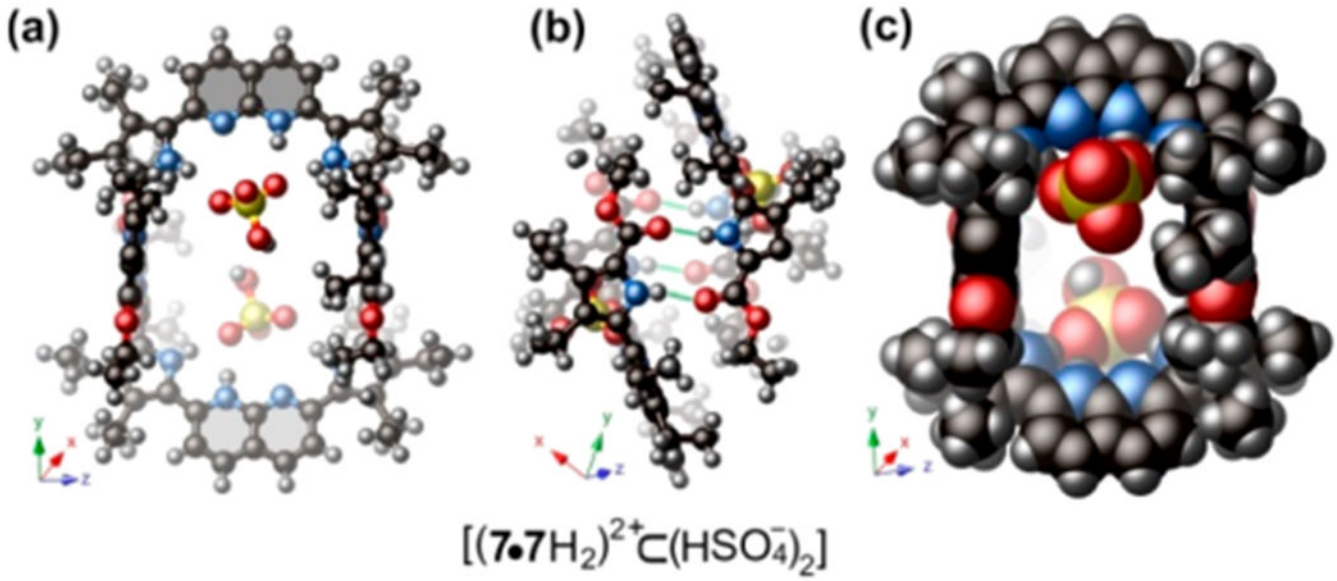

Figure 3.

(a, b) Single crystal X-ray structure of the hydrogen-bonded receptor **7•7** with H_2SO_4, having the empirical chemical formula $[(\mathbf{7}\bullet\mathbf{7}H_2)^{2+}\subset(H_2SO_4^{-})_2]$. (c) Space-filling model of the host–guest complex.

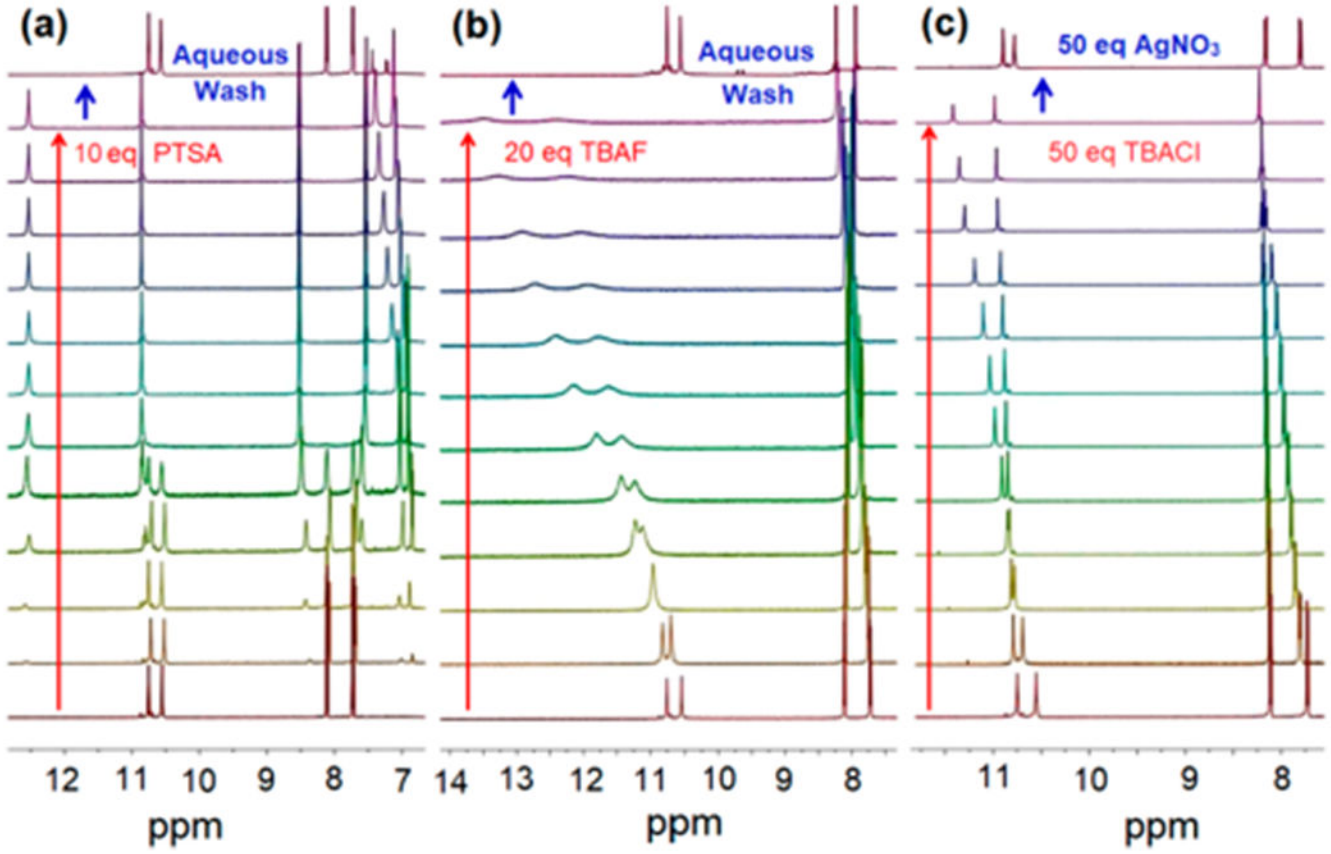

Figure 4.

(a) Changes in the ^{1}H NMR spectrum (partial views) seen when host **7•7** is subject to titration with increasing quantities of PTSA (up to 10 equiv) and after aqueous washing. (b) Changes in the ^{1}H NMR spectrum (partial views) seen when host **7•7** is treated with increasing quantities of TBAF (up to 20 equiv). (c) Changes in the ^{1}H NMR spectrum (partial views) seen when host **7•7** is treated with increasing quantities of TBACl (up to 50 equiv) followed by treatment with $AgNO_3$ (50 equiv). All ^{1}H NMR spectroscopic experiments were performed at 600 MHz in THF-d_8 at 298 K under otherwise identical conditions.

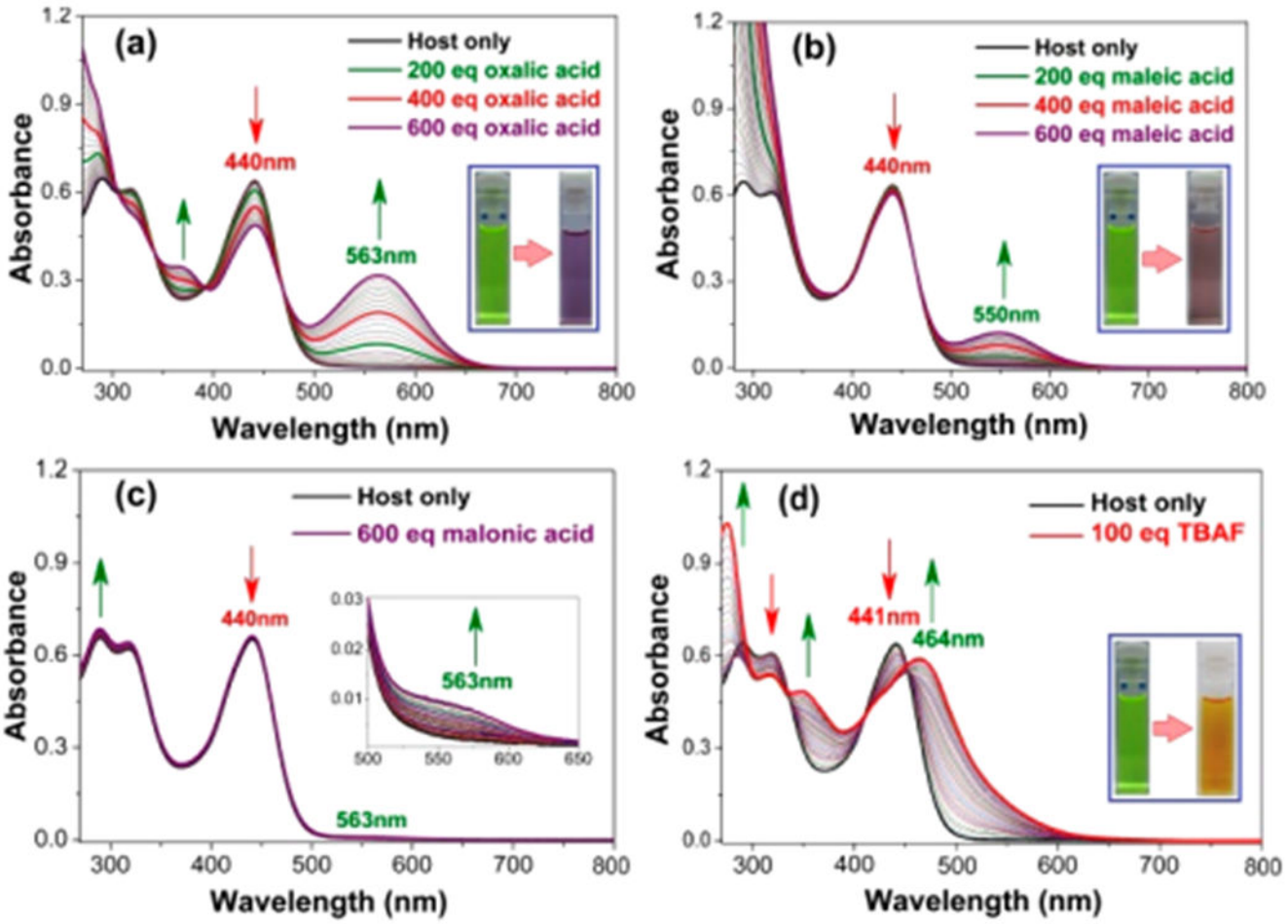

Figure 5.

(a–d) Representative UV–vis spectroscopic titrations showing the changes in the spectral features observed when receptor **7•7** is titrated with increasing quantities of (up to 600 equiv) oxalic acid, maleic acid, malonic acid, and TBAF (100 equiv), respectively. All experiments were carried out with [**7•7**] = 1.00×10^{-5} M in anhydrous THF at 298 K. Insets: Photographs under ambient light of the initial host solution and the corresponding solutions obtained after the addition of the indicated titrants.

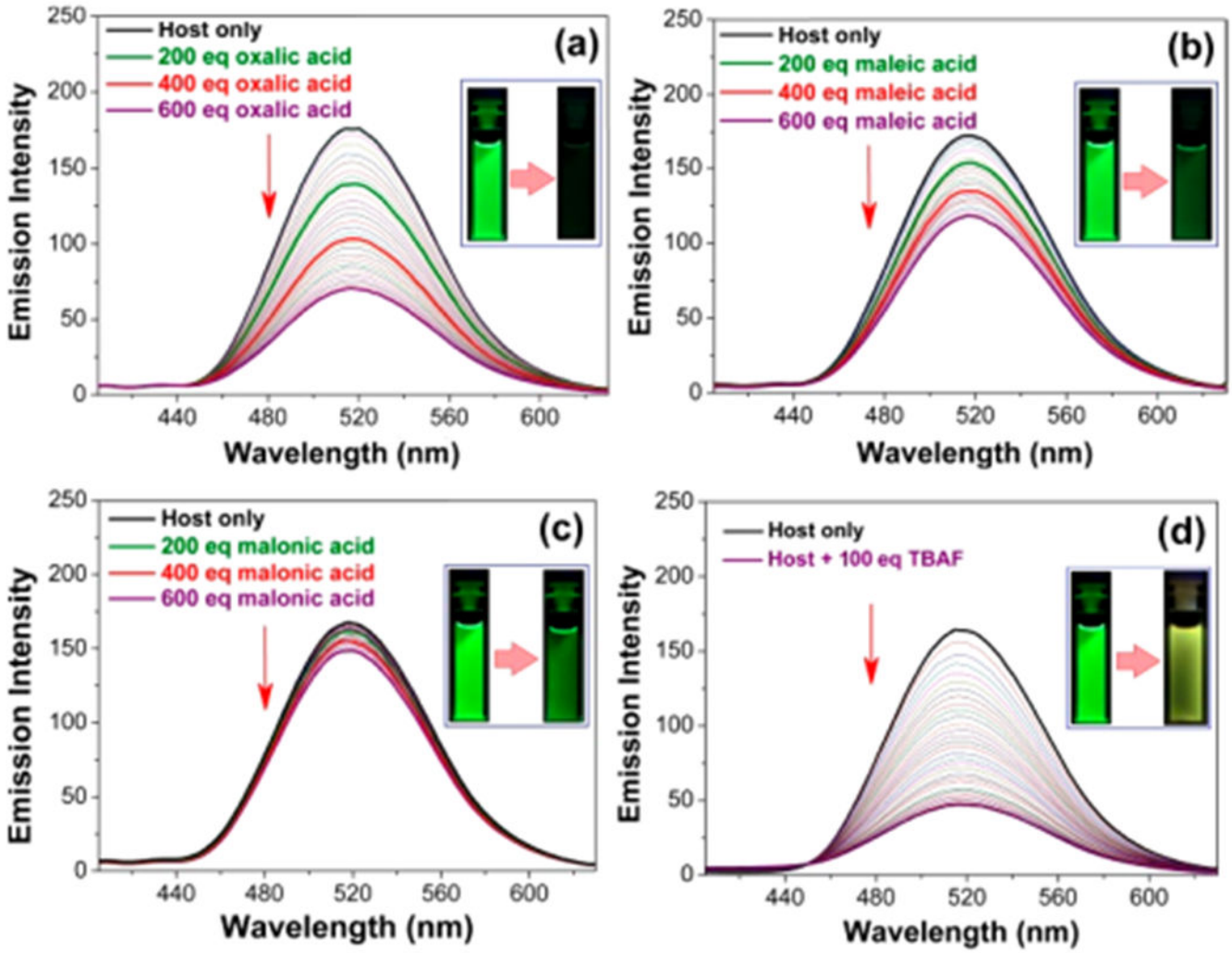

Figure 6.

Emission spectroscopic titrations of **7•7** (1.00×10^{-6} M in anhydrous THF) involving the incremental addition of up to 600 equiv of oxalic acid (a), maleic acid (b), and malonic acid (c), and 100 equiv of TBAF (d) at 298 K. An excitation wavelength (λ_{ex}) of 320 nm was used in all cases. Insets: Photographs of the host-based emission as seen in the presence of the indicated guests with irradiation provided by a 365 nm UV lamp.

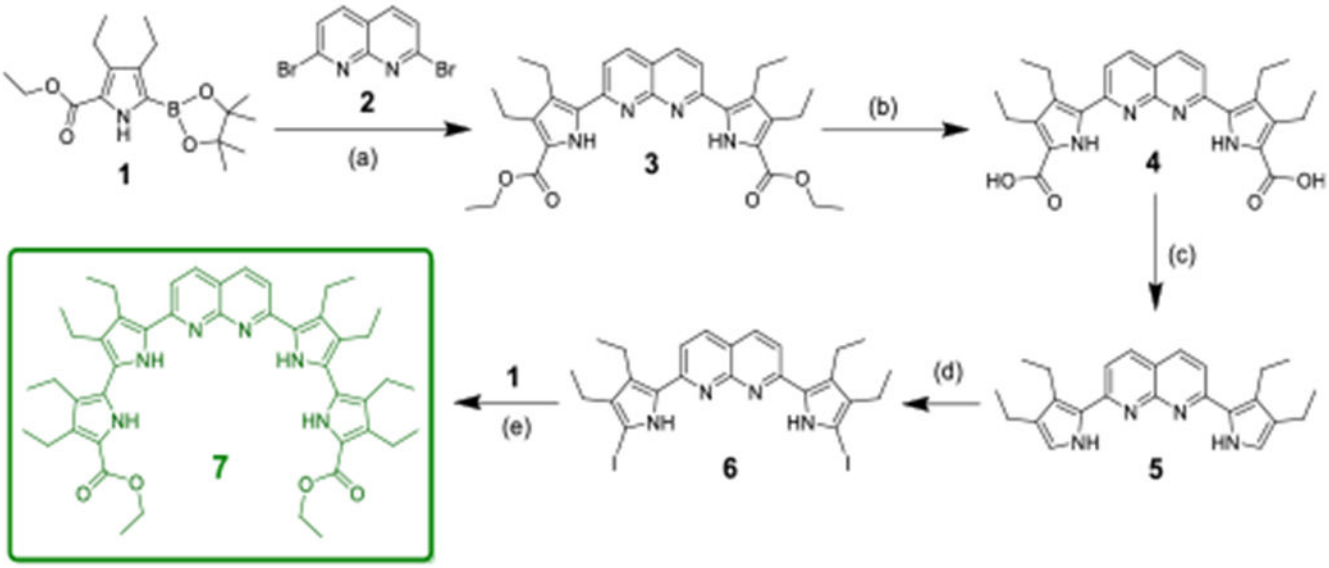

Scheme 1. Synthesis of the Naphthyridine-Containing Tetrapyrrole 7*a*

*a*Reagents, conditions, and yields: (a) $Pd(OAc)_2$, PPh_3, K_2CO_3, DMF/H_2O, N_2, reflux, 24 h (yield: 70%); (b) NaOH, EtOH/H_2O, 85 °C, 5 h (yield 95%); (c) ethylene glycol, 185 °C, 50 min (yield: 91%); (d) I_2/KI, $NaHCO_3$, CH_2Cl_2/H_2O, rt, 1 h, $Na_2S_2O_3$ (yield: 65%); (e) $Pd(PPh_3)_4$, K_2CO_3, DMF/H_2O, reflux, 16 h (yield: 45%).